

Orbital X-ray modulation study of three Supergiant HMXBs

Chetana Jain^{1,2}, Biswajit Paul² and Anjan Dutta¹

¹ Department of Physics and Astrophysics, University of Delhi, Delhi 110007, India;
chetanajain11@gmail.com

² Raman Research Institute, Sadashivnagar, C. V. Raman Avenue, Bangalore 560080, India

Abstract We present the orbital X-ray modulation study of three high mass X-ray binary systems, IGR J18027–2016, IGR J18483–0311 and IGR J16318–4848 using data obtained with *RXTE*-ASM, *Swift*-BAT and *INTEGRAL*-ISGRI. Using the long term light curves of the eclipsing HMXB IGR J18027–2016, obtained with *Swift*-BAT in the energy range 15–50 keV and *INTEGRAL*-ISGRI in the energy range 22–40 keV, we have determined three new mid eclipse times. The newly determined mid eclipse times together with the known values were used to derive an accurate value of the orbital period of 4.5693(4) d at MJD 52168 and an upper limit of $3.9(1.2) \times 10^{-7}$ d d⁻¹ on the period derivative. We have also accurately determined an orbital period of 18.5482(88) d for the intermediate system IGR J18483–0311, which displays an unusual behaviour and shares many properties with the known SFXTs and persistent supergiant systems. This is a transient source and the outbursts occur intermittently at intervals of 18.55 d. Similarly, in the third supergiant system, IGR J16318–4848, we have found that the outbursts are separated by intervals of 80 d or its multiples, suggesting a possible orbital period.

Key words: X-ray: Neutron Stars - X-ray Binaries: individual (IGR J18027–2016, IGR J18483–0311 and IGR J16318–4848)

1 INTRODUCTION

The INTErnational Gamma-Ray Astrophysics Laboratory, *INTEGRAL* was launched in 2002 October (Winkler et al. 2003) and has discovered many new hard X-ray sources during the regular survey of the Galactic center (Revnivtsev et al. 2004, Bird et al. 2007, Kuulkers et al. 2007). In the pre-*INTEGRAL* era, most of the known HMXBs were Be-X-ray binary systems, but the *INTEGRAL* observations have significantly changed the statistics concerning the nature of the companion star of HMXBs. For instance, Liu et al. (2000) had mentioned 54 Be X-ray systems and 7 supergiant X-ray binary systems in their catalog of HMXBs. But, due to a large field of view of the instruments on board *INTEGRAL* (Lebrun et al. 2003, Ubertini et al. 2003), and a high sensitivity at hard X-rays, several new HMXBs have been discovered and the proportion of supergiant systems has increased drastically. It has particularly revealed many new HMXBs which are obscured by the dense and highly absorbing circumstellar wind of the companion, because of which these X-ray sources are not observable at low energies. Bird et al. (2007) identified 68 HMXBs in their third IBIS/ISGRI soft γ -ray survey catalog. Out of these,

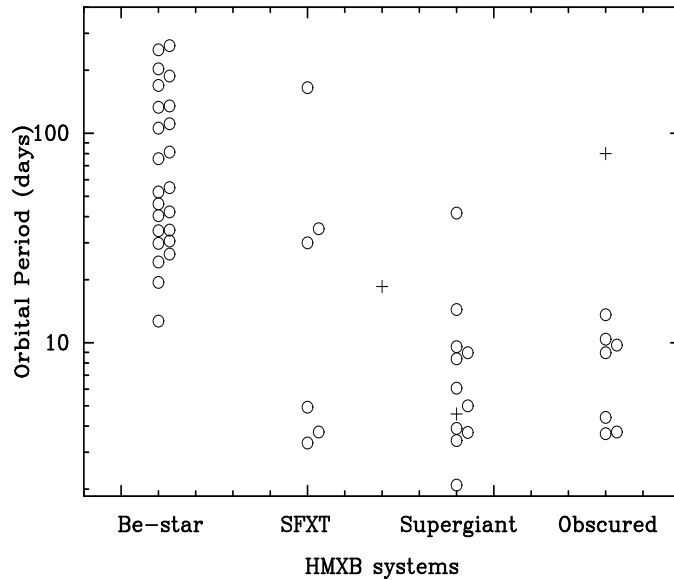


Fig. 1 Orbital period distribution in high mass X-ray binaries categorized into Be-star system, the SFXTs, the persistent supergiants and the obscured sources. The + indicate the orbital period of the three systems studied in the present work.

24 systems were identified as Be X-ray systems and 19 as supergiants. In about 5 years since its launch, *INTEGRAL* has revealed two distinct classes of supergiant X-ray binary systems. The first class includes obscured persistent sources (Kuulkers 2005) and the second class includes sources displaying a short transitory nature (Supergiant Fast X-ray Transients, SFXTs) with outbursts lasting for a few hours (Negueruela et al. 2006, Sguera et al. 2005, 2006). **Further, several persistent low luminosity, slow X-ray pulsators have also been identified, some of which belong to HMXB systems (Kaur et al. 2009).**

Figure 1 shows the orbital period distribution of the different sub-classes of high mass X-ray binaries. We have categorized the distribution into Be-star systems, the SFXTs, the persistent supergiant systems and the obscured systems. Orbital period of only those HMXBs are shown which are mentioned in the HMXB catalogue by Liu et al. (2007). It is clear from the figure that the orbital period in Be-star systems range from 12–262 d, whereas the orbital period of supergiant systems are relatively shorter. The orbital period in these systems are mostly less than 15 d, except for one system having an orbital period of 42 d. Amongst the SFXTs listed in the catalogue, the orbital period is known in six systems and it varies over a wide range of 3.3–165 d. The obscured sources tend to have small orbital periods with the widest known orbital period of about 13 d. The orbital periods of the three sources studied in this work are marked with a “plus” sign. The first source is an intermediate SFXT having an orbital period of about 18 d. The second source is a supergiant HMXB, whereas the third one is a highly obscured system.

We have carried out orbital modulation studies of bright *INTEGRAL* sources and have discovered a very short orbital period in one source, SFXT IGR J16479–4514 (Jain et al. 2009). Here, we present results from three of the brightest *INTEGRAL* sources, IGR J18027–2016, IGR J18483–0311 and IGR J16318–4848. These systems have a late O/early B type supergiant companion and are highly absorbed sources. While IGR J18027–2016 and IGR J18483–0311

are pulsars, nature of the compact object in IGR J16318–4848 is not yet known in spite of extensive observations with different observatories. IGR J18027–2016 is an eclipsing high mass X-ray binary consisting of a neutron star spinning with a period of 139 s. The eclipses provide a good fiducial timing marker for precise determination of the orbital evolution. IGR J18483–0311 is an intermediate system whose position on the Corbet diagram (Corbet 1986) indicates that it is likely a Be system, but a periodic fast X-ray transient activity observed in this system is typical of an SFXT system. It is therefore important to determine its orbital parameters. IGR J16318–4848 is one of the most absorbed Galactic sources known with an enormously high column density. A study of orbital modulation in all these systems is important to understand the mechanism for the short and long duration outbursts and is also useful to plan future orbital phase dependent observations.

IGR J18027–2016 is spatially associated with the X-ray pulsar SAX J1802.7–2017 (Augello et al. 2003) which was serendipitously discovered during a *Beppo*-SAX observation of the LMXB GX 9+1 in 2001 September. It is an eclipsing HMXB system and harbors an X-ray pulsar accreting matter from the stellar wind of the companion star, which is a late O/early B-type supergiant with a mass of 18.8–29.3 M_{\odot} (Hill et al. 2005). From the *Beppo*-SAX observations, Augello et al. (2003) determined a pulse period of 139.612 s and from the pulse arrival time analysis, they determined an orbital period of ~ 4.6 d. It was later confirmed by Hill et al. (2005), who determined an orbital period of 4.5696(9) d from the eclipse timing measurement of the ISGRI data. They also determined a projected semimajor axis ($a_x \sin(i)$) of 68 lt-s and a mass function of 16 M_{\odot} , from which they concluded the mass of the donor to be 18.8–29.3 M_{\odot} and radius of 15.0–23.4 R_{\odot} . Spectral analysis with *XMM-Newton* and *INTEGRAL*-ISGRI indicate a strong intrinsic absorption with a hydrogen column density N_H of 6.8×10^{22} cm^{-2} (Hill et al. 2005). Lutovinov et al (2005) fitted the 18–60 keV spectrum with a powerlaw alongwith an exponential cutoff at high energies ($E_c \sim 18$ keV).

IGR J18483–0311 was discovered with *INTEGRAL* during a survey of the Galactic plane in 2003 April (Chernyakova et al. 2003). An average flux of ~ 10 mCrab in the 15–40 keV was observed, which decreased to 5 mCrab in the 40–100 keV energy range. IGR J18483–0311 is a high mass X-ray binary with an early B-type supergiant companion star (Rahoui et al. 2008). From the timing analysis of the *RXTE*-ASM light curve, Levine et al. (2006) reported a 18.55(5) d orbital period and 21 s X-ray pulsations were reported by Sguera et al. (2007). The source displays an unusual behaviour and shares many properties with the known SFXTs and persistent supergiant systems. Association with a B0.5Ia supergiant companion star (Rahoui et al. 2008) and a fast X-ray transient activity (Sguera et al. 2007), indicate that the system could be an SFXT. But, the outbursts last for a few days, in contrast to a few hours long outbursts seen in other well known SFXTs (Sguera et al. 2007). The quiescent emission level is also higher in IGR J18483–0311, yielding an L_{max}/L_{min} ratio of $\sim 10^3$, whereas, in SFXTs, the ratio is $10^4 - 10^5$. The system is therefore considered to be an “intermediate” SFXT. The 3–50 keV spectra is well fitted by an absorbed powerlaw with a photon index of 1.4 and a cutoff at 22 keV. A high intrinsic absorption is also seen with a column density, N_H of 9×10^{22} cm^{-2} . Spectra during the outbursts is well fit by an absorbed bremsstrahlung with N_H of 7.5×10^{22} cm^{-2} and $kT \sim 21.5$ keV (Sguera et al. 2007).

IGR J16318–4848 is one of the highly obscured Galactic X-ray sources discovered by *INTEGRAL* (Courvoisier et al. 2003) and follow-up by the *XMM-Newton* observatory accurately localized its position (de Plaa et al. 2003, Schartel et al. 2003). A flux of 50–100 mCrab was observed in the 15–40 keV energy band with a significant variability on timescales of more than 1000 s (Walter et al. 2003). Observations made with the *XMM-Newton* revealed the presence of strong Fe- K_{α} , Fe- K_{β} and Ni- K_{α} emission lines (Schartel et al. 2003, de Plaa et al. 2003), alongwith a highly absorbed powerlaw ($\Gamma \sim 1.7$ -2.1) continuum (Matt & Guainazzi 2003). The IR spectrum is also rich in emission lines, various orders of H, He I and He II (Kaplan et al. 2006). IGR J16318–4848 is surrounded by dense circumstellar material and powered by accretion from a stellar wind (Revnivtsev et al. 2003, Filliatre & Chaty 2004). From the archived

ASCA observations, Revnivtsev et al. (2003) determined an enormously high column density, $N_H \simeq 10^{24} \text{ cm}^{-2}$, due to which, the source is not observable at energies below 4 keV.

We report the timing analysis of these three bright supergiant systems, IGR J18027–2016, IGR J18483–0311 and IGR J16318–4848. Using the data obtained from *Swift*-BAT and *INTEGRAL*-ISGRI, we have determined the orbital periods of IGR J18027–2016 and IGR J18483–0311. We have also discovered an 80 d periodicity in the occurrence of outbursts in IGR J16318–4848, which is possibly indicative of a binary orbital period.

2 OBSERVATIONS AND ANALYSIS

We have used data obtained with instruments on board Rossi X-ray Timing Explorer (*RXTE*), *Swift* Gamma Ray Burst Explorer and INTERNATIONAL Gamma-Ray Astrophysics Laboratory (*INTEGRAL*). The three sources were regularly monitored by the All Sky Monitor (ASM) on board the *RXTE*. The ASM data used for the present work covered the time span from MJD 50088 to MJD 54860. The 15–50 keV light curves of IGR J18027–2016, IGR J18483–0311 and IGR J16318–4848 were obtained from the Burst Alert Telescope (BAT; Barthelmy et al. 2005) on board the *Swift* observatory. The observations covered the time range from MJD 53413 to MJD 54867. For all the three sources, the 22–40 keV long term *INTEGRAL*-ISGRI light curve spanned ~ 1350 days.

IGR J18027–2016: The long term *Swift*-BAT, *INTEGRAL*-ISGRI and *RXTE*-ASM light curves of IGR J18027–2016 were corrected for the earth motion using the *earth2sun* tool of the HEASARC software package “Ftools” ver6.5.1. We searched for the orbital period using the *ftool* - *efsearch*, which folds the light curve with a large number of trial periods around an approximate period. Figure 2 shows the *efsearch* result on the light curve of IGR J18027–2016. The top panel shows the result of period search on the long term *Swift*-BAT light curve. The peak here corresponds to the periodicity in the light curve. The inset figure is the expanded view around the peak. A gaussian fit around the peak gave the gaussian center as 394793(103) s (4.5693(11) d). The *efsearch* result of the *INTEGRAL* data, over the same range as in *Swift*-BAT, is shown in the second panel. The main peak corresponds to a period of 395056(210) s (4.5723(24) d). It should be noted that the present *INTEGRAL* dataset is longer than that analyzed by Hill et al. 2005, who determined a period of 4.570 (3) d using the ISGRI data spanning ~ 417 days. The *INTEGRAL* data used in the present work covered the time range from MJD 52698 to MJD 54041. The third panel shows the *efsearch* result on the 5–12 keV *RXTE*-ASM light curve. A peak is present but with a poor significance. The peak corresponds to a period of 394805(185) s (4.5695(21) d).

We have also confirmed the periodicity in the light curves of IGR J18027–2016, using the Lomb-Scargle periodogram method by means of the fast implementation of Press & Rybicki (1989) and Scargle (1982) technique. Figure 3 shows the periodogram generated using the *Swift*-BAT, *INTEGRAL*-ISGRI and *RXTE*-ASM light curves. As seen in Figure 3, a clear peak is present in the periodogram generated from the *Swift* and *INTEGRAL* light curves. But, periodicity could not be confirmed from the *RXTE*-ASM observations. The power spectrum in the case of *Swift*-BAT and *INTEGRAL*-ISGRI data, peaks at 0.218 d^{-1} , which corresponds to a periodicity of 4.5871 d. This result is in sync with the values determined by the *efsearch* analysis and those reported by Hill et al. (2005). The significance of these peaks was confirmed by a randomization test. For both, *Swift*-BAT and *INTEGRAL*-ISGRI light curves, the time stamps of the observed count rates were randomly shuffled and a periodogram was generated from the resulting time series. We simulated 10,000 light curves and determined the maximum power for both the cases. As shown in Figure 3, the horizontal lines in the top two panels show the significance level. The dotted and dashed lines respectively show the 99.9% and 99% significance power among the randomized light curves. This imply that a peak power of 281 and 61 in the original *Swift*-BAT and *INTEGRAL*-ISGRI periodograms is unlikely to occur by chance and therefore the period detection is significant.

Table 1 X-ray mid-eclipse times of IGR J18027–2016.

Cycle	Mid eclipse time (MJD)	Uncertainty (d)	Satellite
0†	52168.26	0.04	<i>Beppo-SAX</i>
68	52478.78	0.12	<i>RXTE-ASM</i>
167†	52931.37	0.04	<i>INTEGRAL-ISGRI</i>
239	53260.37	0.07	<i>INTEGRAL-ISGRI</i>
352	53776.82	0.07	<i>Swift-BAT</i>
511	54503.38	0.07	<i>Swift-BAT</i>

†Reported by Hill et al. 2005

To determine the long term orbital solution, we folded the *Swift*-BAT, *INTEGRAL*-ISGRI and *RXTE*-ASM light curves in 16 phasebins with a period of 394805 s. The folded light curves are shown in Figure 4. A sharp eclipse is clearly seen in the folded *Swift*-BAT light curve. The eclipse lasts for ~ 0.2 orbital phase. A clear eclipse is also seen in the folded *INTEGRAL*-ISGRI light curve but it is not sharp as compared to the eclipse seen in the folded *Swift*-BAT light curve. The eclipse detection in the folded *RXTE*-ASM light curves is not significant, but we emphasize that it occurs at the same phase as seen in the other two observations. We fitted a gaussian to the eclipse phase and the center of the best fit gaussian gives the mid eclipse time for that observation. **From the folded *Swift*-BAT light curve, we determined an eclipse half width of 0.1923 orbital phase. This implies an eclipse half angle of 0.604 radians. The mass of the companion star is known to lie within a range of 19–29 M_{\odot} . Therefore, assuming a canonical mass of 1.4 M_{\odot} for the neutron star, the lower limit on the companion star radius will lie in the range 16.4–24.7 R_{\odot} .**

Table 1 gives a log of the mid eclipse times determined from each observation. We determined two mid eclipse times from the *Swift*-BAT data and one from *INTEGRAL*-ISGRI data. The eclipse seen in the *RXTE*-ASM light curve is not sharp and hence the determination of mid eclipse time involves a large error. We then combined these newly determined mid eclipse times with the known values and fitted a quadratic model to the ephemeris history. We determined an orbital period (P_{orb}) of 394787(34) s (4.5693(4) d) and a period derivative of $3.9(1.2) \times 10^{-7}$ d d $^{-1}$ at MJD 52168. We then subtracted the best fit linear component from the ephemeris history and the residual is plotted in Figure 5. There are only few mid eclipse times reported for this source, therefore, it is not possible to accurately determine the orbital evolution of this binary system. But it should be noted that the period is indeed evolving and probably, future observations of the source can lead to determination of the orbital evolution in this system. **In particular, since this is an eclipsing system, the optical measurements of the companion star can be useful to place a constraint on the rate of mass loss from the donor star.**

IGR J18483–0311: The *efsearch* period search result on the long term *Swift*-BAT, *INTEGRAL*-ISGRI and *RXTE*-ASM light curves of IGR J18483–0311 are shown in Figure 6. Clear peaks are seen in all the three results. A gaussian was fit around the peak in the *Swift*-BAT period search results (inset figure in the top panel) and the peak center determined. An orbital period of 1602796(2268) s (18.550(26) d) was determined. The peak in the *efsearch* result of the 22–40 keV *INTEGRAL*-ISGRI and 5–12 keV *RXTE*-ASM light curves corresponds to 1600227(2989) s (18.521(34) d) and 1602571(767) s (18.5482(88) d), respectively. These results are an improvement over the results obtained by Sguera et al. (2007), who analyzed ~ 1142 days of data from the *INTEGRAL* observations and determined an orbital period of 18.52 d. Whereas, the present result is more complete with the *INTEGRAL* data covering the time range from MJD 52704 to MJD 54053.

IGR J18483-0311 is a bursting source and therefore, initially we could not determine an accurate period from the *efsearch* analysis of the entire *INTEGRAL* light curve. But after

the removal of 5σ bursts (as explained later), we determined the orbital period accurately. We have confirmed the periodicity in the long term *Swift*-BAT and *RXTE*-ASM light curves by using the Lomb-Scargle periodogram technique as mentioned in the case of IGR J18027–2016. As shown in Figure 7, the peak in the Lomb-Scargle periodogram of the *Swift*-BAT light curve corresponds to 0.0538 d^{-1} , .i.e. a period of 18.5873 d. Similarly, from the *RXTE*-ASM light curve (Figure 7, bottom panel) a period of 18.7617 d has been found. The dotted and the dashed horizontal lines in Figure 7 correspond to 99.9% and 99% significance level as determined from the randomization test explained before. The *Swift*-BAT, *INTEGRAL*-ISGRI and *RXTE*-ASM light curves were folded into 32 phasebins with a period of 1602571 s and are shown in Figure 8. Clear peaks are seen in all the three folded light curves. The folded light curve shows that the source is inactive for about half the orbit.

IGR J18483–0311 is a transient source and many outbursts have been recorded by the instruments on board *INTEGRAL*. Figure 9 shows the long term *INTEGRAL*-ISGRI light curve binned with an orbital period of 18.5482 d. The bottom panel of the same figure shows the long term light curve binned with a period one-sixteenth of the orbital period. Large variations, akin to the SFXT outbursts are seen in the bottom panel compared to the light curve shown in the top panel. To determine their phase occurrence, we took the light curve binned with 1.1592 d and assuming a uniform exposure throughout the observation, we divided the signal count rate by the error associated with it. The resulting light curve is shown in Figure 10 (top panel). We then took the outbursts above 5σ and 10σ level and considering an orbital period of 18.5482 d, we determined their phase of occurrence with respect to the most intense outburst. A histogram of the number of outburst in each orbital phase was created. It is shown in the bottom panel of Figure 10. The solid curve in the histogram corresponds to outburst above 10σ level and the dotted curve is for the 5σ level. As can be seen in the figure, most of the outbursts occur at the same phase as the reference “most intense” outburst. Although, a few outburst occur at other phases also, but this result confirms the periodicity in the occurrence of outbursts.

After the removal of 5σ bursts, we searched for an orbital period in the *INTEGRAL* data and the *efsearch* result is shown in Figure 6 (middle panel). The folded *INTEGRAL* light curve, after the removal of 5σ outbursts, is shown in Figure 8 (middle panel). The profile is similar to the folded profile obtained of the *Swift*-BAT and the *RXTE*-ASM light curves.

IGR J16318–4848: As done in the case of IGR J18027–2016 and IGR J18483–0311, the long term *Swift*-BAT, *INTEGRAL*-ISGRI and *RXTE*-ASM light curves were first corrected for the earth motion and the periodicity was searched using the ftool *efsearch*. The period search results are shown in Figure 11. Top panel shows the *efsearch* result from the *Swift*-BAT light curve and a peak is seen near $\sim 7 \times 10^6$ s. The period search analysis in IGR J16318–4848 is being reported for the first time, therefore, we have searched for a period over a wide range of trial periods. The inset figure is the expanded view around the peak, about which we fit a gaussian model. We obtained the best fit gaussian center as 6931624(1202) s (80.227(14) d). The detection significance of periodicity from the *INTEGRAL* and *RXTE* observations is very small, but we do detect a peak at 6915874(1808) s (80.045(21) d) and 6929084(1912) s (80.198(22) d), respectively. We tried to confirm the periodicity using the Lomb-Scargle periodogram technique as done above for the other two sources, but we could not detect a significant peak.

Figure 12 shows the folded *Swift*-BAT, *INTEGRAL*-ISGRI and *RXTE*-ASM light curves of IGR J16318-4848. The light curves were folded with the respective best period determined in each case. We have done the rest of the analysis with the *Swift*-BAT light curve, which has the best statistics amongst the three observations. A clear peak is seen in the folded light curve, along with small secondary peaks. The main peak lasts for about 0.2 orbital phase. Figure 13 shows the *Swift*-BAT light curve binned with a binsize of 80.22 d. The bottom panel of the same figure shows the light curves binned with a binsize one-sixteenth of 80.22 d. An intense outburst near the end of the observation clearly stands out and the peak observed in the folded orbital light curve could be dominated by this.

To check this, we applied a similar analysis as done above for IGR J18483-0311. We divided the signal count rate by the error in rate determination for the light curve binned with 5.013 d (shown in Figure 14 (top panel)). We then took the outbursts above 15σ and 20σ level and considering an orbital period of 80 d, we determined the phase of occurrence of outbursts with respect to the most intense outburst. The bottom panel of Figure 14 shows the histogram of number of outbursts in each phase. Most of the outbursts occur around an orbital phase of 0.1, with occasional outbursts at phases about 0.4 and 0.7. It implies that though the outbursts occur with a periodicity of ~ 80 d, there are three different orbital phases at which they occur.

3 DISCUSSION

Using the long term *Swift*-BAT, *INTEGRAL*-ISGRI and *RXTE*-ASM data of IGR J18027–2016, we have determined an accurate value of the orbital period of 4.5693(4) d. From the *Swift*-BAT and *RXTE*-ASM data, we have accurately determined an orbital period of 18.5482(88) d for IGR J18483–0311 and have found that the outbursts occur intermittently at intervals of ~ 18.55 d. We have also found a ~ 80 d periodicity in the occurrence of outbursts from IGR J16318–4848.

All the three sources, IGR J18027–2016, IGR J18483–0311 and IGR J16318–4848, studied in the present work, are bright supergiant High Mass X-ray Binaries which accrete material through the stellar wind of a late O/early B-type supergiant companion. The classical supergiant systems have small and circular orbits, as compared to relatively larger orbits found in Supergiant Fast X-ray Transients. However, there are exceptions to this. Recently, Jain et al. (2009) determined a 3.32 d orbital period for the SFXT system IGR J16479–4514, which is smaller than that known in other SFXTs, IGR J11215–5952 (165 d: Romano et al. 2007; Sidoli et al. 2007) and SAX J1818.6–1703 (30 d: Bird et al. 2009). An orbital period of 4.56 d for IGR J18027–2016 is well within the expected range for supergiant systems, but an orbital period of 18.5508 d determined for IGR J18483–0311, is somewhat more than that expected from a supergiant system. IGR J18483–0311 is active for about half the orbital cycle. The quiescent emission level in IGR J18483–0311 is also higher (Sguera et al. 2007). All this imply that the source is an intermediate system between classical supergiants and SFXTs.

IGR J16318–4848 is a highly absorbed source with a hydrogen column density, $N_H \simeq 10^{24} \text{ cm}^{-2}$. The presence of strong absorption shows that the compact object must be embedded in a dense circumstellar envelope, originating from the accretion of stellar winds. **In several HMXBs, the orbital periods have been determined either through the timing analysis of the X-ray data (example, IGR J16479–4514: Jain et al. (2009); IGR J17544–2619: Clark et al. (2009); IGR J17252–3616: Zurita Heras et al. (2006)) or through the timing of the recurrent outbursts (example IGR J11215–5952: Sidoli et al. (2007); SAX J1818.6–1703: Sidoli et al. (2009)).** We have studied the periodicity in the occurrence of outbursts in this system. The periodicity of ~ 80 d in the outburst behaviour most likely represents the orbital period of the binary system and is a key diagnostic for studying the geometry of the system.

Several models have been proposed to explain the occurrence of periodic outbursts in the supergiant systems. In’t Zand (2005) suggested the “clumpy winds” model according to which the wind from the donor star is composed of dense clumps with mass of the order of $10^{19} - 10^{20}$ g (Howk et al. 2000). Neutron star accretes from the wind of the supergiant at different rates depending on the wind density and short flares occur due to episodic accretion of clumps from the massive winds. Negueruela et al. (2008) suggested that outbursts occur due to accretion of clumps from the spherical wind. They proposed that the orbit of these systems are large and the wind clumps density is small. The outbursts in IGR J16318–4848 have been observed to occur at different orbital phases. **The pattern of the X-ray outbursts depend on the size, eccentricity and the orientation of the orbit.** Sidoli et al. (2007) proposed that the

supergiant wind has an “equatorial disk” component, in addition to the spherically symmetric polar component. Outbursts occur when the neutron star crosses the equatorial disk component at the periastron, which is denser than the polar wind component. The neutron star can cross the disk twice depending on the truncation of the disk, its orientation and inclination with respect to the orbital plane.

In view of the results presented above, we point out that more sensitive and frequent monitoring of all the three sources is required in order to understand them in detail. Specially in the case of IGR J18027–2016, which show clear eclipses which can be used to time mark the orbital modulation and determine the orbital evolution in the system, if any. Using longer data sets, we have been able to determine the orbital period of IGR J18483–0311 with greater accuracy. Regular monitoring of the absorbed source IGR J16318–4848 is important to detect the orbital period with confidence.

ACKNOWLEDGMENTS

We thank the *Swift*-BAT and *RXTE*-ASM teams for provision of the data

References

- Augello G., Iaria R., Robba N. R., Di Salvo T., Burderi L., Lavagetto G., Stella L., 2003, *ApJ*, 596, L63
- Barthelmy S. D., Barbier L. M., Cummings J. R. et al., 2005, *Space Science Reviews*, 120, 143
- Bird A. J., Malizia A., Bazzano A. et al., 2007, *ApJS*, 170, 175
- Bird A. J., Bazzano A., Hill A. B., McBride V. A., Sguera V., Shaw S. E., Watkins H. J., 2009, *MNRAS*, 393, L11
- Chernyakova M., Lutovinov A., Capitanio F., Lund N., Gehrels, N., 2003, *ATel*, 157, 1
- Clark D. J., Hill A. B., Bird A. J., McBride V. A., Scaringi S., Dean A. J., 2009, arXiv 0908.1041**
- Corbet R. H. D., 1986, *MNRAS*, 220, 1047
- Courvoisier T. J. L., Walter R., Rodriguez J., Bouchet L., Lutovinov A. A., 2003, *IAUC*, 8063, 3
- de Plaa J., den Hartog P. R., Kaastra J. S., in’t Zand J. J. M., Mendez M., Hermsen W., 2003, *ATel*, 119, 1
- Filliatre P., Chaty S., 2004, *ApJ*, 616, 469
- Hill A. B., Walter R., Knigge C. et al., 2005, *A&A*, 439, 255
- Howk J. C., Cassinelli J. P., Bjorkman J. E., Lamers H. J. G. L. M., 2000, *ApJ*, 534, 348
- in’t Zand J. J. M., 2005, *A&A*, 441, L1
- Jain C., Paul B., Dutta A., 2009, ***MNRAS*, 397, L11**
- Kaplan D. L., Moon D. S., Reach W. T., 2006, *ApJ*, 649, L107
- Kaur R., Wijnands R., Patruno A. et al., 2009, *MNRAS*, 394, 1597**
- Kuulkers E., 2005, *AIPC*, 797, 402
- Kuulkers E., Shaw S. E., Paizis A. et al., 2007, *A&A*, 466, 595
- Lebrun F., Leray J. P., Lavocat P. et al., 2003, *A&A*, 411, L141
- Levine A. M., Corbet R., 2006, *ATel*, 940, 1
- Liu Q. Z., van Paradijs J., van den Heuvel E. P. J., 2000, *A&AS*, 147, 25
- Liu Q. Z., van Paradijs J., van den Heuvel E. P. J., 2006, *A&A*, 455, L1165
- Lutovinov A., Revnivtsev M., Gilfanov M., Shtykovskiy P., Molkov S., Sunyaev R., 2005, *A&A*, 444, 821
- Matt G., Guainazzi M., 2003, *MNRAS*, 341, L13

- Negueruela I., Smith D. M., Reig P., Chaty S., & Torrejon J. M., 2006, *ESASP*, 604, 165
- Negueruela I., Torrejon J. M., Reig, P., Ribo, M., Smith, D. M., 2008, *AIPC*, 1010, 252
- Press W. H., Rybicki G. B., 1989, *ApJ*, 338, 277
- Rahoui F., Chaty, S., Lagage P., Pantin E., 2008, *A&A*, 484, 801
- Revnivtsev M. G., Sazonov S. Yu., Gilfanov M. R., Sunyaev R. A., 2003, *AstL*, 29, 587
- Revnivtsev M. G., Sunyaev R. A., Varshalovich D. A. et al., 2004, *AstL*, 30, 382
- Romano P., Sidoli L., Mangano V., Mereghetti S., Cusumano G., 2007, *A&A*, 469, L5
- Scargle J. D., 1982, *ApJ*, 263, S835
- Schartel N., 2003, *IAUC*, 8072, 3
- Sguera V., Barlow E. J., Bird A. J., et al., 2005, *A&A*, 444, 221
- Sguera V., Bazzano A., Bird A. J., et al., 2006, *ApJ*, 646, 452
- Sguera V., Hill A. B., Bird A. J., et al., 2007, *A&A*, 467, 249
- Sidoli L., Romano P., Mereghetti S., Paizis A., Vercellone S., Mangano V., Gotz D., 2007, *A&A*, 476, 1307
- Sidoli L., Romano P., Esposito P. et al. 2009, arXiv 0907.4041**
- Ubertini P., Lebrun F., Di Cocco G., et al., 2003, *A&A*, 411, L131
- Walter R., 2003, *A&A*, 411, L427
- Winkler C., Courvoisier T. J. L., Di Cocco G., et al., 2003, *A&A*, 411, L1
- Zurita Heras J. A., de Cesare G., Walter R., Bodaghee A., Belanger G., Courvoisier T. J. L., Shaw S. E., Stephen J. B. 2006, A&A, 448, 261**

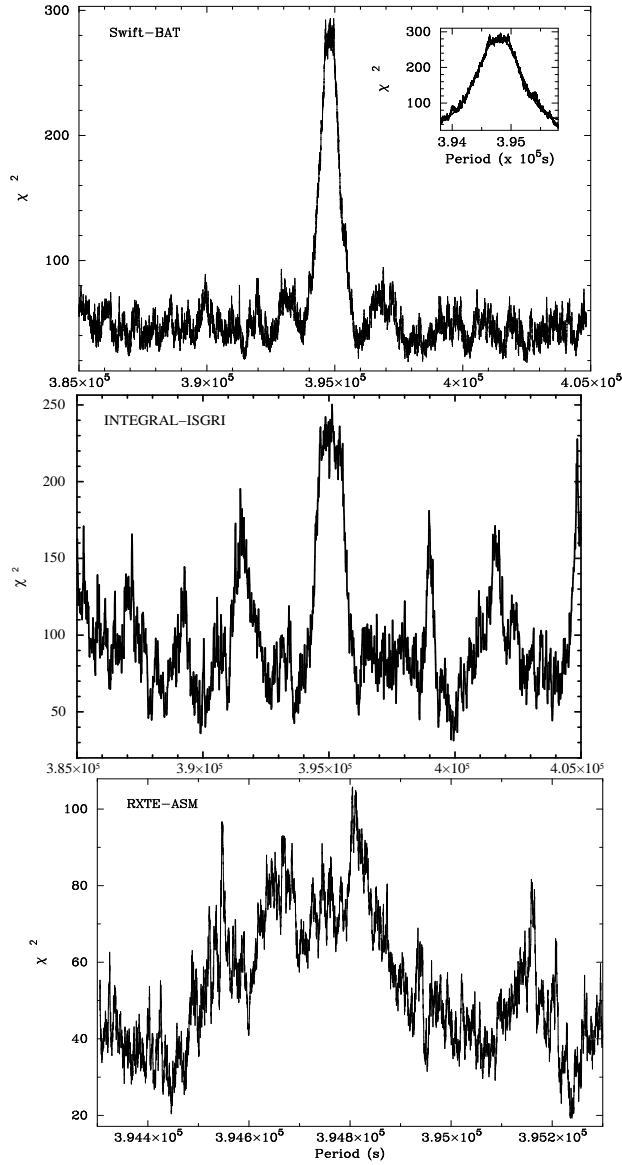


Fig. 2 Result from *efsearch* on the light curve of IGR J18027–2016. The top panel shows the result from the *Swift*-BAT observations and the inset figure shows the expanded view around the peak. The solid line represents the best fit gaussian curve with the centre at 394793(103) s. The second and third panels show the *efsearch* results from *INTEGRAL*-ISGRI and *RXTE*-ASM light curves. The peak in the *INTEGRAL*-ISGRI result corresponds to a period of 395056(210) s, while from the *RXTE*-ASM data, we determined a period of 394805(185) s.

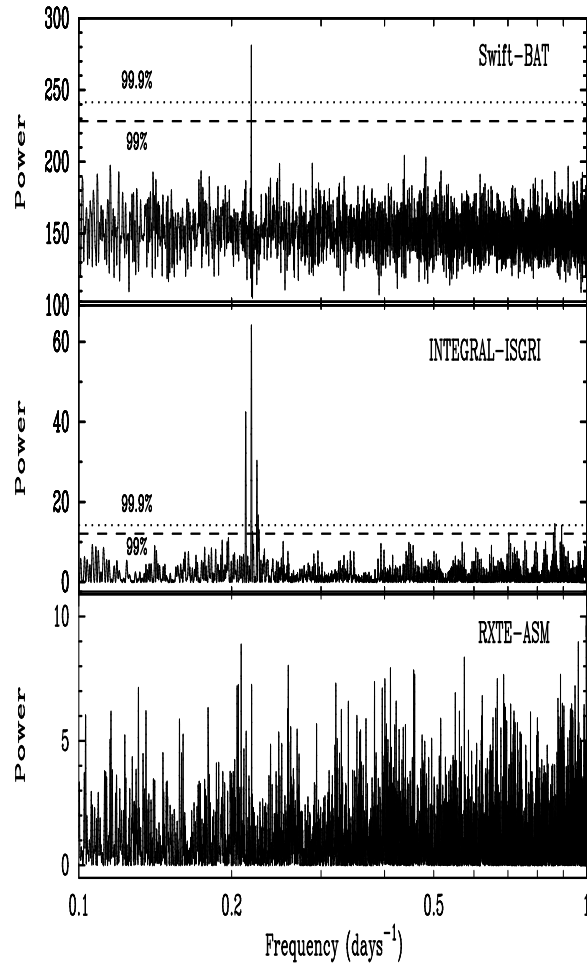


Fig. 3 The Lomb-Scargle periodogram generated from the *Swift*-BAT, *INTEGRAL*-ISGRI and *RXTE*-ASM light curves of IGR J18027–2016. The highest peak in the top and the middle panels correspond to a frequency of 0.218 d^{-1} , i.e. a period of 4.5871 d.

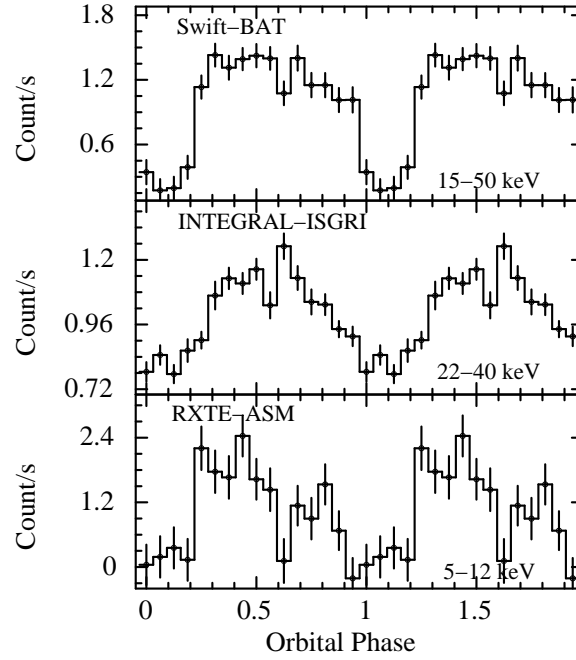


Fig. 4 The light curve of IGR J18027–2016 folded in 16 bins with a period of 394805 s. The folded light curves of *Swift*-BAT, *INTEGRAL*-ISGRI and *RXTE*-ASM observations are shown in the top, middle and bottom panels respectively.

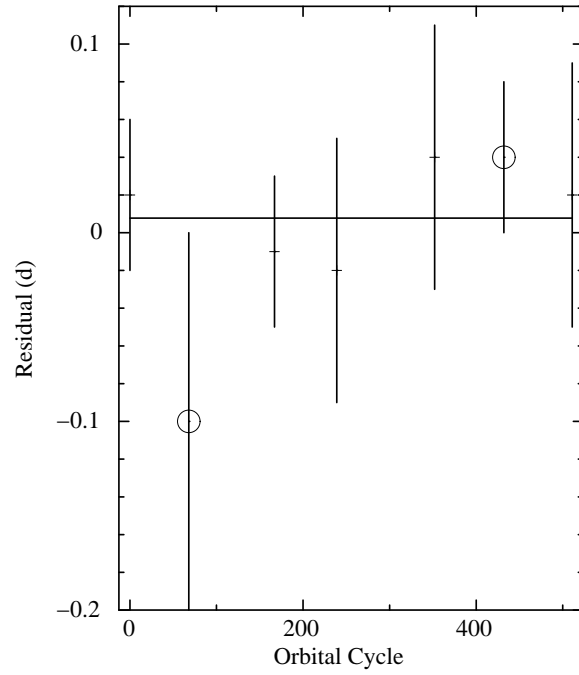


Fig. 5 The mid eclipse time residuals of IGR J18027–2016 are plotted as a function of the orbital cycle, relative to the best fit linear ephemeris ($P_{orb} = 4.5693$ d at MJD 52168). The mid eclipse times are tabulated in Table 1. The “o” represents the *RXTE*-ASM and average *Swift*-BAT, respectively.

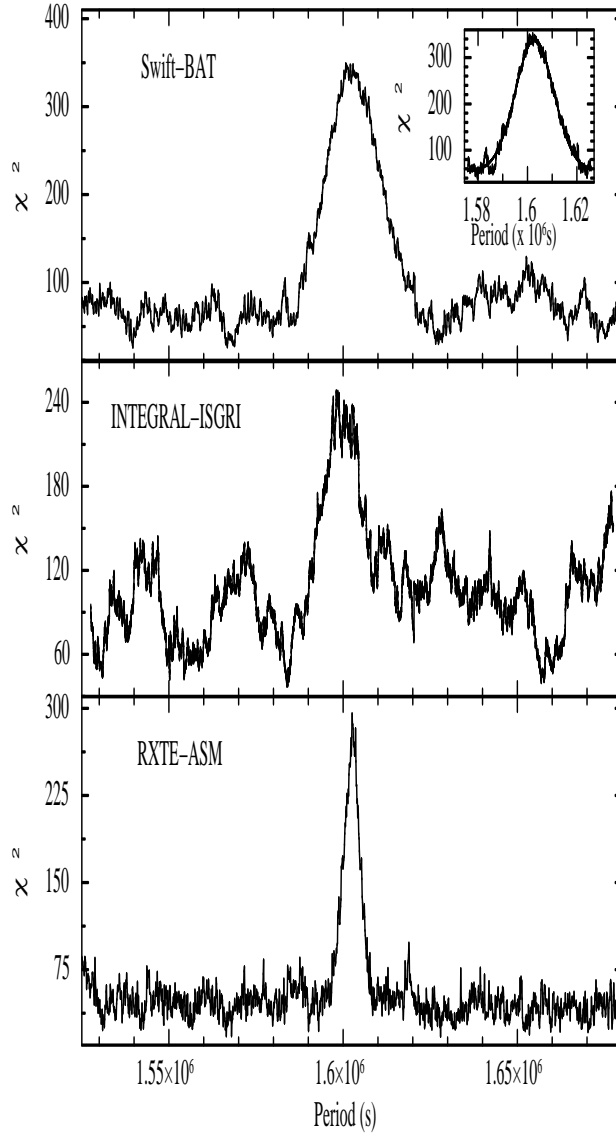


Fig. 6 Results from *efsearch* on the light curve of IGR J18483–0311. The top, middle and bottom panels show the result from the *Swift*-BAT, *INTEGRAL*-ISGRI and *RXTE*-ASM observations, respectively. The inset figure in the top panel shows the expanded view around the peak determined from the *Swift*-BAT observations. The solid line represents the best fit gaussian curve with the centre at 18.550(26) d. The peaks in the *INTEGRAL*-ISGRI and *RXTE*-ASM results respectively correspond to a period of 18.521(34) d and 18.5482(88) d.

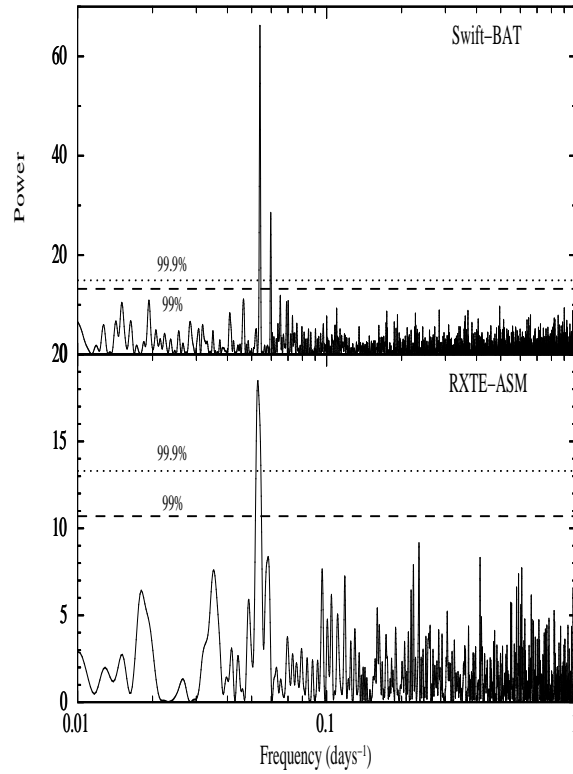


Fig. 7 The Lomb-Scargle periodogram generated from the *Swift*-BAT and *RXTE*-ASM light curves of IGR J18483–0311, are respectively shown in the top and the bottom panel. The peak in the top panel corresponds to a frequency of 0.0538 d^{-1} , i.e. a period of 18.5873 d. The peak in the periodogram generated from the *RXTE* data corresponds to a frequency of 0.0533 d^{-1} , i.e. a period of 18.7617 d.

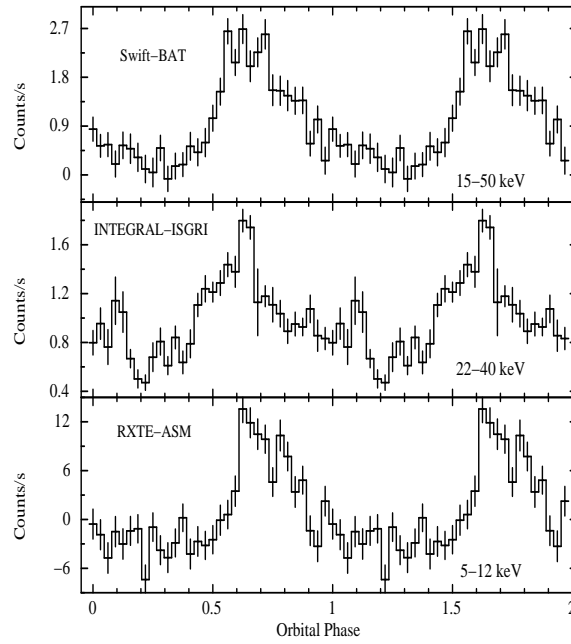


Fig. 8 The light curve of IGR J18483–0311 folded into 32 bins with a period of 1602571 s. The top, middle and bottom panels, respectively show the folded light curves of *Swift*-BAT, *INTEGRAL*-ISGRI and *RXTE*-ASM observations.

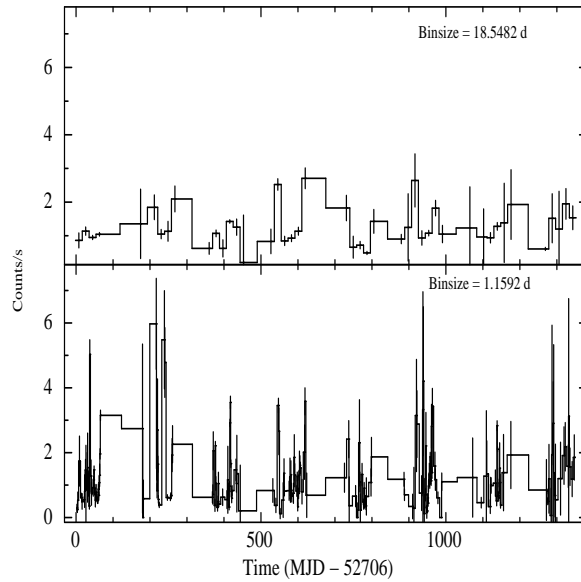


Fig. 9 The long term light curve of IGR J18483-0311, binned with binsize of 18.5482 d and 1.1592 d.

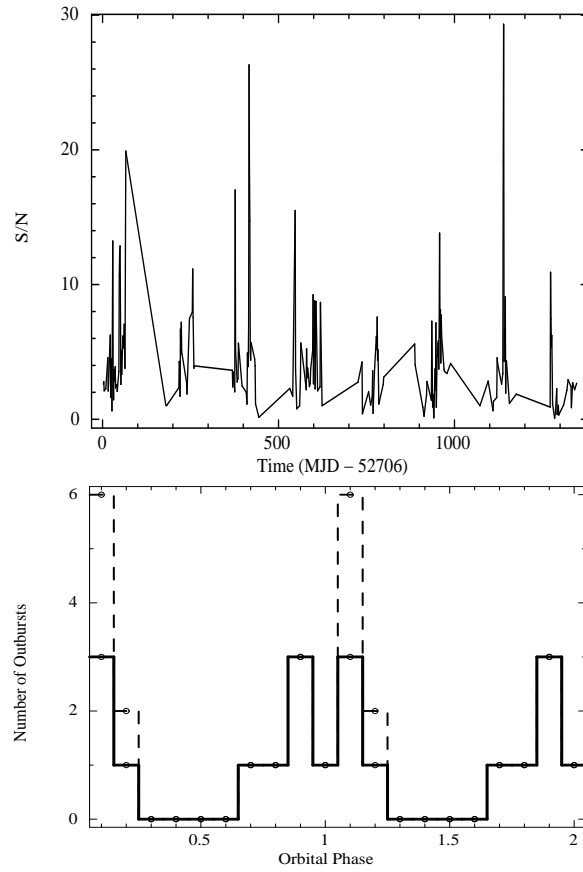


Fig. 10 The *Swift*-BAT light curve of IGR J18483–0311, binned with a binsize of 1.1592 d. The count rate was divided by the error. The bottom panel shows the histogram of number of outbursts with respect to the orbital phase. The dashed line shows the number of outbursts above the 5σ level and solid line shows the number of outbursts above the 10σ level.

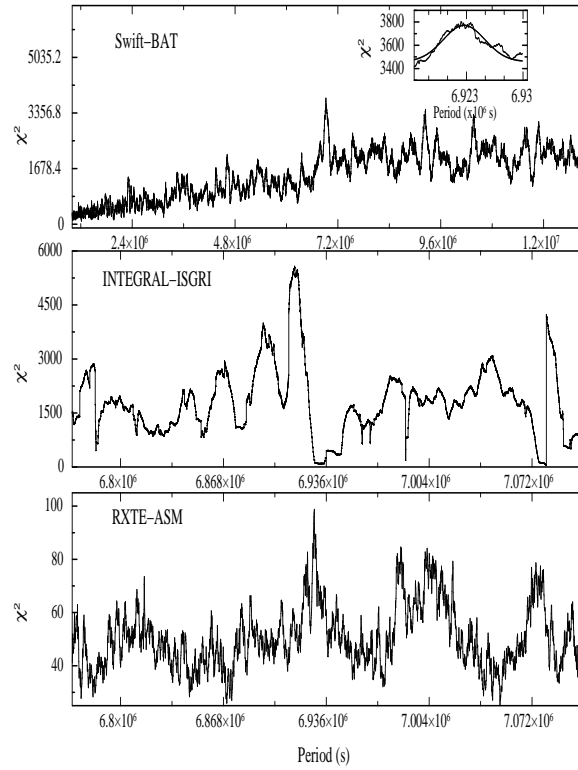


Fig. 11 Results from *efsearch* on the light curve of IGR J16318–4848. The top panel shows the result from the *Swift*-BAT observations, over a wide range of trial periods. The inset figure shows the expanded view around the peak determined from the *Swift*-BAT dataset. The solid line represents the best fit gaussian curve with the centre at 80.227(14) d. The middle and the bottom panels show the *efsearch* result near the peak from the *INTEGRAL* and *RXTE*-ASM data. The peaks correspond to 80.045(21) d and 80.198(22) d, respectively.

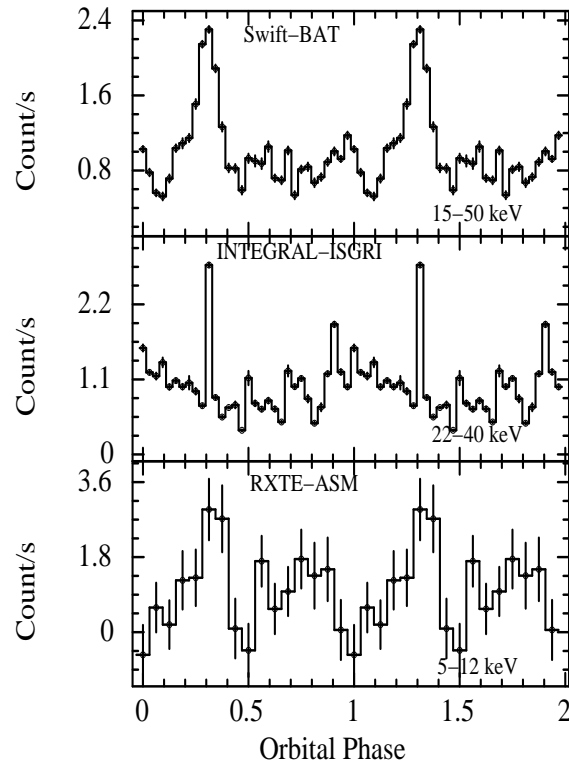


Fig. 12 The folded *Swift*-BAT, *INTEGRAL*-ISGRI and *RXTE*-ASM light curves of IGR J16318-4848. The light curves were folded with the respective best period determined in each case.

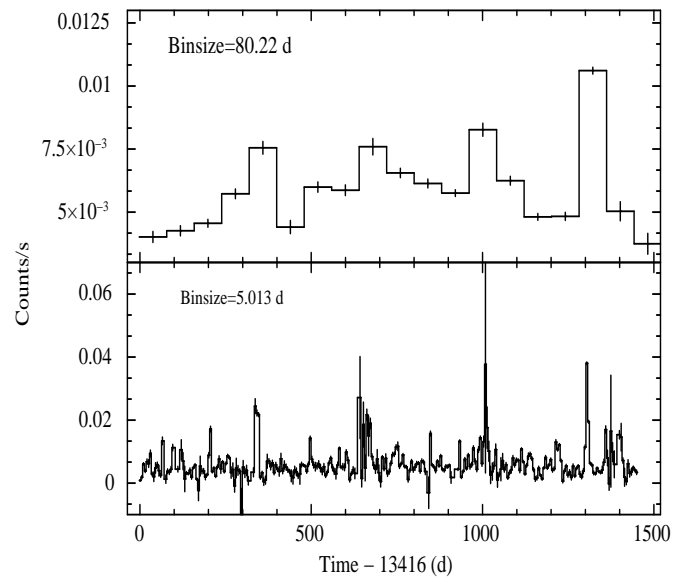


Fig. 13 The long term light curve of IGR J16318–4848, binned with binsize of 80.22 d and 5.013 d.

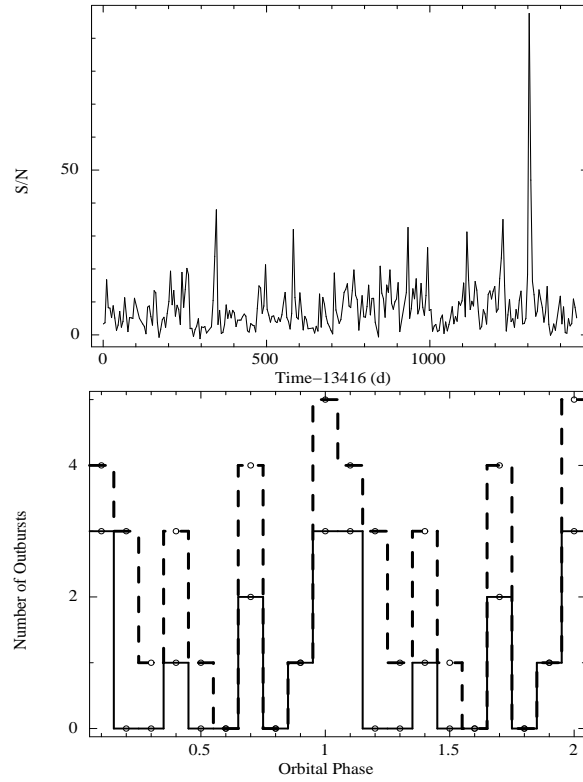


Fig. 14 The *Swift*-BAT light curve of IGR J16318–4848, binned with a binsize of 5.013 d. The count rate was divided by the error. The bottom panel shows the histogram of number of outbursts with respect to the orbital phase. The dashed line shows the number of outbursts greater than 15σ and solid line shows the number of outbursts greater than 20σ level.